doi:10.1016/j.jmb.2010.12.013 J. Mol. Biol. (2011) 406, 1–8

Contents lists available at www.sciencedirect.com

Journal of Molecular Biology

journal homepage: http://ees.elsevier.com.jmb

COMMUNICATION

Structural Basis for Human PHF2 Jumonji Domain Interaction with Metal Ions

John R. Horton†, Anup K. Upadhyay†, Hideharu Hashimoto, Xing Zhang and Xiaodong Cheng*

Department of Biochemistry, Emory University School of Medicine, Atlanta, GA 30322, USA

Received 25 October 2010; received in revised form 1 December 2010; accepted 2 December 2010
Available online 15 December 2010

Edited by R. Huber

Keywords:
epigenetics;
histone lysine demethylation;
PHF2;
Epe1;
methyl-lysine binding

PHF2 belongs to a class of α-ketoglutarate-Fe^{2+}-dependent dioxygenases. PHF2 harbors a plant homeodomain (PHD) and a Jumonji domain. PHF2, via its PHD, binds Lys4-trimethylated histone 3 in submicromolar affinity and has been reported to have the demethylase activity of monomethylated lysine 9 of histone 3 *in vivo*. However, we did not detect demethylase activity for PHF2 Jumonji domain (with and without its linked PHD) in the context of histone peptides. We determined the crystal structures of PHF2 Jumonji domain in the absence and presence of additional exogenous metal ions. When Fe^{2+} or Ni^{2+} was added at a high concentration (50 mM) and allowed to soak in the preformed crystals, Fe^{2+} or Ni^{2+} was bound by six ligands in an octahedral coordination. The side chains of H249 and D251 and the two oxygen atoms of *N*-oxalylglycine (an analog of α-ketoglutarate) provide four coordinations in the equatorial plane, while the hydroxyl oxygen atom of Y321 and one water molecule provide the two axial coordinations as the fifth and sixth ligands, respectively. The metal binding site in PHF2 closely resembles the Fe^{2+} sites in other Jumonji domains examined, with one important difference—a tyrosine (Y321 of PHF2) replaces histidine as the fifth ligand. However, neither Y321H mutation nor high metal concentration renders PHF2 an active demethylase on histone peptides. Wild type and Y321H mutant bind Ni^{2+} with an approximately equal affinity of 50 μM. We propose that there must be other regulatory factors required for the enzymatic activity of PHF2 *in vivo* or that perhaps PHF2 acts on non-histone substrates. Furthermore, PHF2 shares significant sequence homology throughout the entire region, including the above-mentioned tyrosine at the corresponding iron-binding position, with that of *Schizosaccharomyces pombe* Epe1, which plays an essential role in heterochromatin function but has no known enzymatic activity.

The PHF2 gene is located on human chromosome 9q22,[1] within a region where alterations of a cluster of genes including PHF2 are associated with a wide variety of tumors.[2] PHF2 belongs to a small family of Jumonji proteins with three members (PHF2, PHF8, and KIAA1718).[3] Each of these proteins harbors two domains in its respective N-terminal half (Fig. 1a): a plant homeodomain (PHD) that binds trimethylated histone H3 lysine 4 (H3K4me3)—a modification associated with transcriptional activation—and their linked Jumonji domains, which remove methyl marks that are associated with transcriptional repression. These activities

*Corresponding author. E-mail address: xcheng@emory.edu.

† J.R.H. and A.K.U. contributed equally to this work.

Abbreviations used: PHD, plant homeodomain; H3K4me3, Lys4-trimethylated histone 3; NOG, *N*-oxalylglycine; ITC, isothermal titration calorimetry.

include the demethylation of di- and monomethylated histone H3 lysine 9 (H3K9me2/1) via PHF8,[4–7] H3K27me2/1 via KIAA1718,[4,8,9] H4K20me1 via PHF8,[10,11] and monomethylated lysine 9 of histone 3 via PHF2.[12] These three proteins share 71% identity among their PHDs, 48% identity among

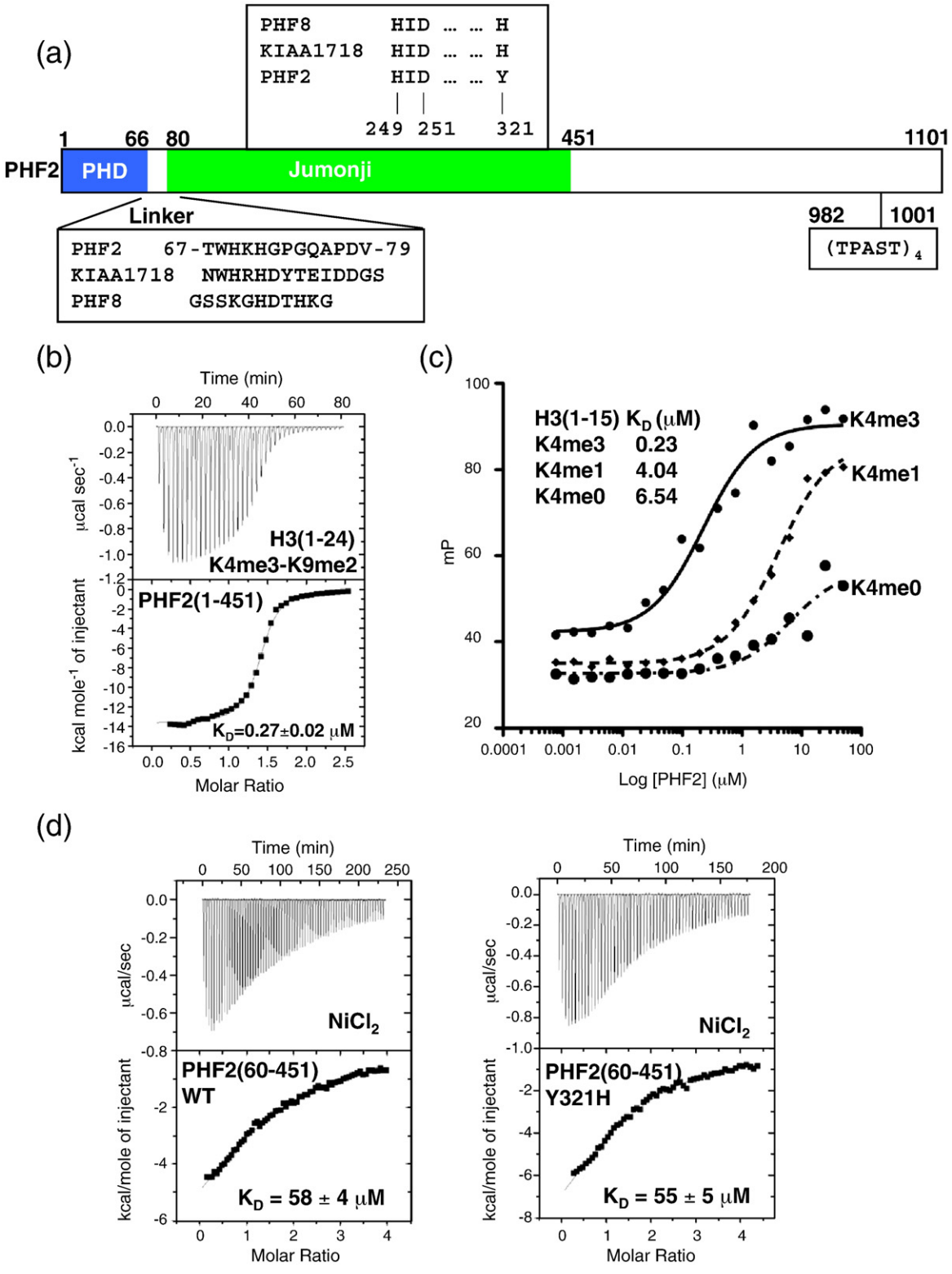

Fig. 1 (*legend on next page*)

their Jumonji domains, and much less conservation among their C-terminal halves with large insertions and deletions (Supplementary Fig. S1). The linker sequences between the PHD and Jumonji domain are not well conserved in sequence or length, although the PHF2 linker is more similar to that of KIAA1718 (Fig. 1a). In addition, PHF2 has the unique sequence of four repeats of TPAST towards the C terminus.

Jumonji domain proteins are a class of α-ketoglutarate-Fe(II)-dependent dioxygenases. Two histidines and one aspartate or glutamate [i.e. the Hx(D/E)…H motif] within the Jumonji domain bind to the ferrous iron. However, a few of them, including mouse and human PHF2 (Y321) and *Schizosaccharomyces pombe* Epe1 (Y370), have a tyrosine at the position corresponding to the distal second iron-binding histidine (Supplementary Fig. S2). Epe1 modulates the stability of silent chromatin in fission yeast,[13] and the Epe1 protein can be modeled after the structure of FIH (factor-inhibiting hypoxia inducible factor),[14] a protein asparagine hydroxylase that also contains a Jumonji-like domain.[15] Epe1 was proposed to be a putative histone demethylase that could act by oxidative demethylation.[14] However, recombinant Epe1 purified from Sf9 cells lacks histone lysine demethylase activity,[16] whereas functional characterization *in vivo* suggested that Epe1 is involved in changes in methylation patterns of H3K4 and H3K9.[13] This raises the question of whether PHF2, which, like Epe1, contains a tyrosine at the position corresponding to the distal iron-binding histidine, is an active histone demethylase (although it was reported that PHF2 demethylates monomethylated lysine 9 of histone 3 *in vivo*, detected by immunostaining of cells expressing GFP-tagged PHF2 with anti-H3K9me antibodies[12]). Here, we focus on residues 1–451 from PHF2 (containing PHD and Jumonji) and 60–451 (Jumonji) (Supplementary Fig. S3a), comparing their metal binding with that of PHF8 and KIAA1718.

PHF2 Binds H3K4me3

PHF2 (1–451), containing both the PHD and Jumonji domain, binds the histone peptide containing H3K4me3, in agreement with the observation that the PHD alone is capable of binding of H3K4me3 peptide,[12] with a K_D of approximately 0.23–0.27 μM measured by isothermal titration calorimetry (ITC) (Fig. 1b) and fluorescence polarization (Fig. 1c). The binding affinity is comparable to that of KIAA1718 (0.29 μM) and stronger by a factor of 4 compared to that of PHF8 (0.95 μM).[4] Neither the length of H3 peptide (1–15 *versus* 1–24 residues) nor the status of H3K9 methylation (me2 *versus* me0) affects the binding affinity (Fig. 1b and c). However, we were not able to detect any *in vitro* demethylation activity of PHF2 by mass spectrometry-based assay[4] on histone peptides containing H3K4me3/2, H3K9me3/2/1, H3K18me2, H3K27me3/2/1, H3K36me3/2/1, H4K20me2, H3R2me2, as well as p53 peptides containing K370me3 and K382me2 (Supplementary Fig. S4a and b) under the reaction conditions established for PHF8 and KIAA1718 [37 °C in 50 mM Hepes (pH 8.0), 50 μM $(NH_4)_2FeSO_4$, 1 mM α-ketoglutarate, and 2 mM ascorbic acid].[4] Furthermore, we varied pH (5.6–11.6), NaCl concentration (50–250 mM), temperature (Supplementary Fig. S4c), and iron concentration (see below) with no activity observed for PHF2.

Structures of PHF2 Jumonji Domain in the Absence and Presence of Metal Ion

Previously, we showed that PHF8 and KIAA1718 expressed and purified from *Escherichia coli* contain iron in the active site without addition of exogenous metal ions.[4] The side chains of the HxD…H motif and two oxygen atoms of α-ketoglutarate or *N*-oxalylglycine (NOG; the cofactor analog) coordinate the binding of the metal ion. In order to elucidate the property of metal binding by PHF2, we crystallized PHF2 Jumonji domain (Supplementary Fig. S3b) in the absence of additional metal ions or in the presence of either Fe^{2+} or Ni^{2+} at high concentrations. Three structures were solved at resolutions of 1.9–2.0 Å in space group $P2_1$ (containing two molecules in the crystallographic asymmetric unit) in the presence of NOG (Supplementary Table S1). The protein components of the structures are highly similar, with a root mean squared deviation (rmsd)

Fig. 1. PHF2 binding of H3K4me3. (a) Schematic representation of PHF2. The linker sequences and the iron binding residues of the family members are indicated (see Supplementary Fig. S1). (b) ITC measurement of binding of PHF2(1–451) to doubly methylated H3(1–24)K4me3-K9me2 peptides, carried out under the conditions of 25 μM protein concentration and 0.35 mM peptide concentration in 20 mM Hepes (pH 8.0), 200 mM NaCl, and 0.25 mM TCEP [tris(2-carboxyethyl) phosphine], using the MicroCal VP-ITC instrument at 25 °C. Binding constant was calculated by fitting the data to one-site binding model equation using the ITC data analysis module of Origin 7.0 (OriginLab Corporation). (c) Dissociation constants as determined by fluorescence polarization with C-terminal fluoresceinated peptides. K_D values are shown. The measurements were carried out at 25 °C on a Beacon 2000 Fluorescence Polarization System (PanVera). A constant amount (5 nM) of H3(1–15)K4me0/1/3 was incubated for 30 min with increasing amounts of proteins in 20 mM Tris-Cl (pH 7.5), 200 mM NaCl, 5% glycerol, and 1 mM dithiothreitol. Curves were individually fit using GraphPad PRISM 5.0c software (GraphPad Software, Inc.). One-site specific binding model equation was used to fit the data: $mP = mP_{baseline} + mP_{max} \times [PHF2]/(K_D + [PHF2])$. (d) ITC measurement of binding of PHF2(60–451) wild type (left) and Y321H mutant (right) to $NiCl_2$ under the conditions of a protein concentration of 54 μM for the wild type or 52 μM for the Y321H and 1 mM $NiCl_2$ in 20 mM Hepes (pH 8.0), 200 mM NaCl, and 5% glycerol.

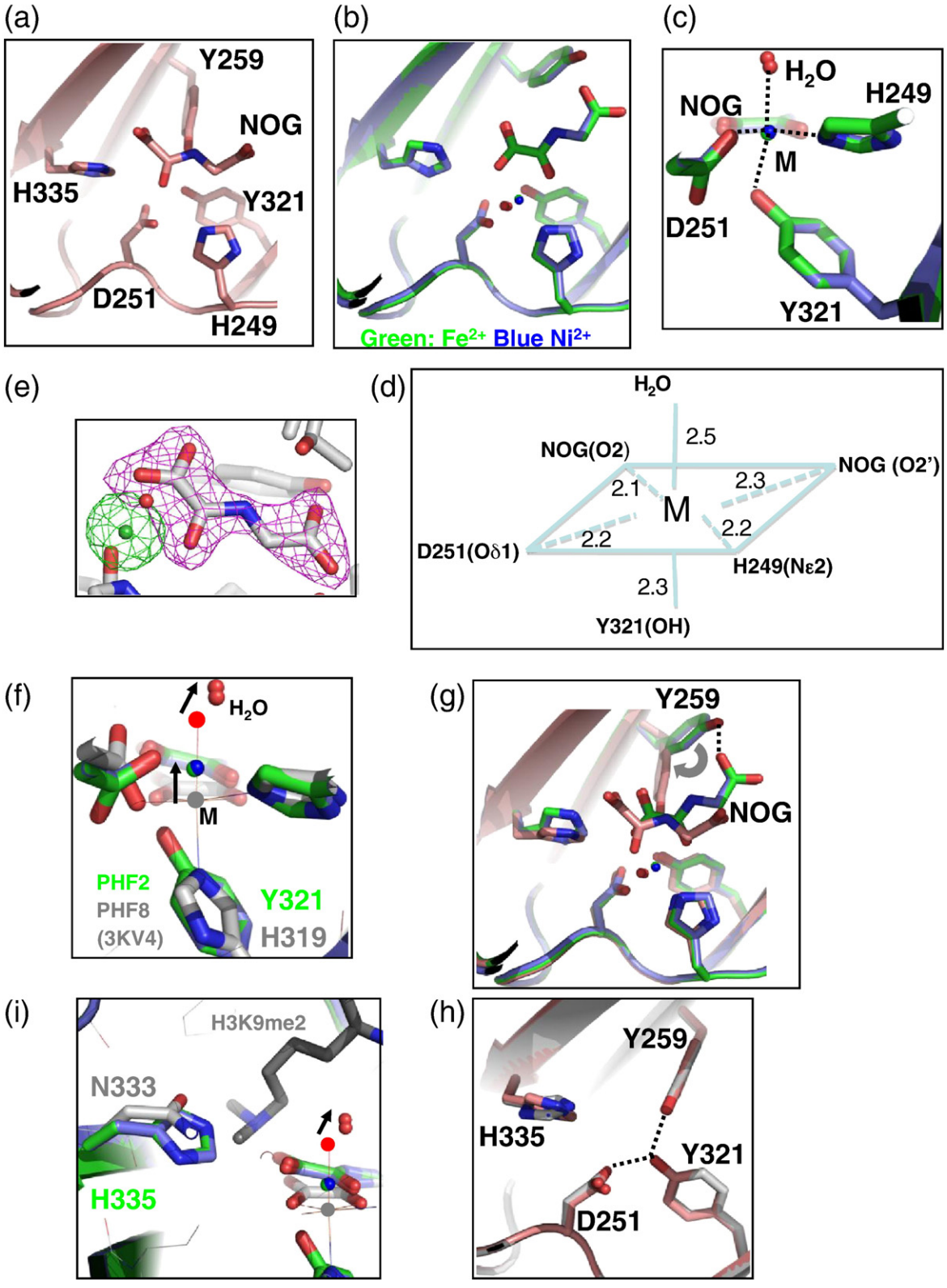

Fig. 2 (*legend on next page*)

of approximately 0.5 Å when comparing 362 pairs of C^{α} atoms. The PHF2 structure is also highly similar to that of PHF8 (rmsd of 1.5 Å) and KIAA1718 (rmsd of 1.2 Å). In addition, we solved the structure of PHF2 without any cofactor in space group $P2_12_12_1$ (one molecule per asymmetric unit) and PHF2-Ni^{2+}-NOG in space group $C2$ (one molecule). Here, we will mainly describe the three structures in $P2_1$ space group (without metal or with bound Fe^{2+} or Ni^{2+}) in the presence of NOG and will discuss the differences among the five structures.

In the absence of exogenous metal ions, no metal was observed in the "active site" of PHF2 (Fig. 2a). Even when a significant amount of metal, 5–10 times of protein concentration (2.5–10 mM *versus* 0.5–1 mM protein concentration), was added during crystallizations or to preformed crystals, no metal was observed (date not shown). We added fresh solutions of iron(II) ammonium sulfate $[(NH_4)_2Fe(SO_4)_2]$ or nickel(II) chloride $[NiCl_2]$ so that their final concentrations were approximately 50 mM in drops containing preformed crystals and allowed these to soak for at least 4 h before flash-freezing the crystals. The drops also contained 100 mM ascorbic acid to keep the metal in the +2 oxidation state. Both Fe^{2+} and Ni^{2+} ions have six ligands in an octahedral coordination (Fig. 2b–e). The side chains of H249 and D251 of the HxD motif and the two oxygen atoms of NOG provide four coordinations in the equatorial plane. The hydroxyl oxygen atom of Y321 and one water molecule provide the two axial coordinations as the fifth and sixth ligands, respectively (Fig. 2d). Substitution of the first ion-binding histidine of the HxD motif to tyrosine (H514Y)[17] or alanine (H514A)[18] in histone H3K4 demethylase JARID1C/SMCX abolishes its enzymatic activity.

The metal binding site in PHF2 closely resembles the Fe^{2+} sites in other Jumonji domains examined, with one small but potentially important difference (Fig. 2f). With a tyrosine in the place of the fifth ligand, the longer side chain of Y321 of PHF2 makes the Fe^{2+} move away from the corresponding binding site in PHF8 (Fig. 2f), an active demethylase. Along with this iron movement, there is a water molecule at the position of the sixth ligand, which is occupied by an O_2 molecule during a reaction that hydroxylates the methyl group of the methyl-lysine substrate. The small movement of the ferrous iron, induced by the presence of Y321, could position the oxygen in a nonreactive mode, such as with decreased oxygen binding affinity in a manner analogous to the distal H58Y mutation in hemoglobin. In that case, the tyrosine becomes the fifth heme ligand in the mutant hemoglobin, which remains in the T configuration with lower oxygen affinity (R.E. Dickerson and I. Geis, 1983. Hemoglobin: Structure, Function, Evolution, and Pathology. The Benjamin/Cummings Publishing Company, Inc., Menlo Park, CA).

Surprisingly, when the structures of PHF2 are compared with and without metal binding in the active site, there is little difference between the conformations of the three protein side-chain ligands. Instead, the absence of metal causes NOG to be displaced from the binding site because Y259 assumes a different rotomer conformation (Fig. 2g). The hydroxyl group of Y259 forms a hydrogen bond with NOG when a metal ion is bound (Fig. 2g). In the absence of a bound metal ion, NOG is displaced and the Y259 hydroxyl group forms a new hydrogen bond with Y321. This same rotomer of Y259 is also observed in the absence of any bound cofactor (i.e., the structure of $P2_12_12_1$) (Fig. 2h). The corresponding tyrosine (Y259 of PHF2) is conserved in PHF8 (Y257) and KIAA1718 (Y292) as well as in JHDM1 (Y222),[19] and their rotomer conformations observed are correlated with cofactor binding (see Supplementary Fig. S12 of Ref. 4).

Superimposition of active sites of PHF8 and KIAA1718 to that of PHF2 indicates that H335 of PHF2 substitutes N333 of PHF8 (or N368 of KIAA1718), which is adjacent to the substrate methyl-lysine binding site (Fig. 2i). In the structure of the PHF8-H3K9me2 complex, the side chain of N333 is in close contact with one of the methyl groups

Fig. 2. Structures of PHF2 Jumonji domain. (a) Active site of PHF2-NOG (brown) in the absence of metal binding. (b) Superimposition of active sites of PHF2-NOG-Fe^{2+} (green) and PHF2-NOG-Ni^{2+} (blue). The metal ions are shown in small balls (Fe^{2+} in green and Ni^{2+} in blue). The water molecules are shown in red small balls. (c) Close-up view of metal (Fe^{2+} or Ni^{2+}) ions binding with six ligands in an octahedral coordination. (d) The octahedral coordination of Fe^{2+} or Ni^{2+} observed in PHF2–NOG–metal interactions. The numbers indicate the distance in angstrom between interacting atoms. (e) Omit electron densities, $F_{obs} - F_{cal}$, contoured at 10σ and 4σ above the mean, are shown for the Fe^{2+} (green mesh) and NOG (magenta mesh), respectively. (f) Superimposition of PHF2-NOG-metal (Fe^{2+} and Ni^{2+} depicted by green and blue small balls, respectively) and the PHF8-NOG-Fe^{2+}-H3K9 peptide complex (PDB 3KV4; Fe^{2+} represented by a grey small ball). PHF2 is shown in color, whereas PHF8 is in grey. The water molecules (labeled as H_2O) are shown as red small balls. The arrows indicate the relatively small movements of the metal (labeled by letter M) and metal-bound water molecule between PHF2 and PHF8. (g) Y259 of PHF2 adopts two conformations. Y259–NOG interaction is observed in the presence of metal ion. The rotation of Y259 side chain (as indicated by a curved arrow) is accompanied by the displacement of NOG from the binding sire in the absence of metal ion. (h) The Y259–Y321 interaction is also observed in the structure of PHF2 without any cofactor (space group $P2_12_12_1$ in Supplementary Table S1). (i) H335 of PHF2 is in the position of N333 of PHF8, which interacts with one of the methyl groups of H3K9me2. The arrow indicates the relatively small movement of the metal-bound water molecule between PHF2 and PHF8, as in panel (f).

of H3K9me2.[4] The bulkier and more rigid side chain of H335 of PHF2 might not allow the binding of a dimethyl-lysine in the corresponding location and, thus, could limit PHF2 as a monomethyl-lysine specific demethylase.

Y321H Mutant neither Alters Metal Affinity nor Restores Histone Demethylation Activity

To test the hypothesis that the catalytic inactivity of PHF2 is due to the tyrosine (Y321) replacement of a histidine as the metal ligand, we cloned and expressed the reverse Y321H mutant of PHF2(60–451). The mutant protein was purified following a three-column chromatography similar to that used for the wild-type protein (see Supplementary Methods), except with 1 mM EDTA (ethylenediaminetetraacetic acid) in the buffer of the first two columns. In the absence of EDTA, the mutant protein, but not the wild type protein, precipitated throughout purification. EDTA-treated Y321H protein remained stable, even after EDTA was removed by size-exclusion chromatography, and was used to measure the protein's affinity for metal by ITC. The results indicate that both wild type and Y321H mutant exhibit the same affinities towards Ni^{2+} with K_D values of approximately 50 μM (Fig. 1d). We have also attempted to measure the K_D of Fe^{2+} ion binding to the PHF2 and its Y321H mutant proteins. However, the propensity of Fe^{2+} to oxidize to Fe^{3+} in oxygenated buffers made these experiments difficult. To stop Fe^{2+} from getting oxidized, we added 20 mM ascorbic acid in the protein buffer and in the Fe^{2+} solution in the syringe. However, titration data generated by this approach show high background signal in the absence of protein, indicating possible reactions involving the Fe^{2+}/oxygen/ascorbic acid triad.

Considering the possibility that PHF2 may require higher metal ion concentration in the reaction buffer (due to its week metal binding affinity) to catalyze demethylation reaction *in vitro*, we have tested the activity of the wild-type as well as Y321H mutant PHF2 proteins in reaction buffers containing 50 μM, 10 mM, or 50 mM $(NH_4)_2Fe(SO_4)_2$ (concentration used for soaking the crystals) with H3 peptides containing K9me2/1 as potential substrates. However, we observed no indication of the lysine demethylase activity of either wild type or Y321H mutant of PHF2 (data not shown). As positive controls, we tested catalytic activities of KIAA1718 under the same conditions using the same substrate peptides.

Discussion

Both PHF8 and KIAA1718 are active enzymes that remove methyl groups from mono- and di-methyl lysines of H3K9 and/or H3K27.[4] Wen *et al.* suggested that PHF2 is capable of removing a methyl group from monomethylated H3K9 *in vivo*,[12] although we were unable to confirm this observation *in vitro*. In an independent study, PHF2 shows no histone demethylase activity on itself but appears to antagonize a transcriptional repressor[20] [i.e., to prevent the demethylation of H3K4me3 by demethylase KDM2B (also known as JHDM1B/FBXL10)].[21]

The variable linker between the PHD and Jumonji domain is a determinant for the relative positioning of the two domains in PHF8 and KIAA1718 that are mainly responsible for substrate specificity.[4] PHF8 adopts a bent conformation, allowing each of its domains to engage its respective target (H3K4me3 or H3K9me2/1), whereas KIAA1718 adopts an extended conformation, which positions its Jumonji domain to access H3K27me2/1 when its PHD engages H3K4me3. The sequence and length of the PHF2 linker, being more similar to that of KIAA1718 (Fig. 1a), might position its two domains in an extended conformation that engages two methyl marks separated further apart in *cis* on the same peptide. Alternatively, the two domains can engage their respective targets in *trans*, as shown in PHF8 whose Jumonji domain also functions as an H4K20me1 demethylase while its PHD interacts with H3K4me3 in the context of chromatin.[10,11]

Besides mammalian PHF2 and *S. pombe* Epe1, the residues important for Fe^{2+} binding are substituted in *Saccharomyces cerevisiae* Gis1 (with a Tyr replacing the distal His), in *S. pombe* Lid2 (with TxS in the positions of HxD), in human JARID2 (with S and V replacing the two histidines, respectively), and in human and mouse Hairless proteins (with a Cys replacing the first His).[3] Among them, *S. pombe* Lid2 is enzymatically active as a trimethyl H3K4 demethylase *in vivo*.[22] It remains to be shown whether Lid2 is an active demethylase *in vitro* and the identities of the Fe^{2+} binding residues. On the other hand, having the perfect match to the consensus sequence of Fe^{2+} binding residues, FIH is a protein asparagine hydroxylase[15] and JMJD6 was (mis)characterized initially as a histone arginine demethylase,[23] later as a protein lysine hydroxylase of RNA splicing-related proteins,[24,25] and more recently was even suggested to modify single-strand RNA.[26] One would wonder whether PHF2 (as well as Epe1) could have different enzymatic activity on non-histone substrates.

Lastly, all three members of the family, PHF2, PHF8, and KIAA1718, contain a serine- and threonine-rich sequence towards the C-terminal end. Particularly, PHF2 contains three or four repeats of TPAST and related TPNTT and SPSTS (Supplementary Fig. S1). *In vitro* kinase assays showed that CDK1 phosphorylates PHF8.[10] We speculate that phosphorylation of PHF2 could potentially stimulate PHF2 demethylase activity in the context of chromatin *in vivo*.

PDB accession numbers

The coordinates and structure factors have been deposited with accession numbers 3PTR (PHF2 Jumonji), 3PU3 (PHF2-NOG), 3PU8 (PHF2-NOG-Fe^{2+}), and 3PUA and 3PUS (PHF2-NOG-Ni^{2+}) in *C*2 and $P2_1$ space group, respectively.

Acknowledgements

The Department of Biochemistry at the Emory University School of Medicine supported the use of the SER-CAT synchrotron beamline at the Advanced Photon Source of Argonne National Laboratory, local X-ray facility, and matrix-assisted laser desorption/ionization time-of-flight mass spectrometry. This work was supported by grant GM068680 to X.C. from the US National Institutes of Health. X.C. is a Georgia Research Alliance Eminent Scholar. J.R.H. performed crystallographic work; A.K.U performed mass spectrometry-based demethylation assays and ITC binding assays; H.H. performed cloning, mutagenesis, and fluorescence polarization assay; X.Z. and X.C. organized and designed the scope of the study; and X.C. wrote the manuscript; all were involved in the analysis of data and helped in revising the manuscript.

Supplementary Data

Supplementary data to this article can be found online at doi:10.1016/j.jmb.2010.12.013

References

1. Hasenpusch-Theil, K., Chadwick, B. P., Theil, T., Heath, S. K., Wilkinson, D. G. & Frischauf, A. M. (1999). PHF2, a novel PHD finger gene located on human chromosome 9q22. *Mamm. Genome*, **10**, 294–298.
2. Sinha, S., Singh, R. K., Alam, N., Roy, A., Roychoudhury, S. & Panda, C. K. (2008). Alterations in candidate genes PHF2, FANCC, PTCH1 and XPA at chromosomal 9q22.3 region: pathological significance in early- and late-onset breast carcinoma. *Mol. Cancer*, **7**, 84.
3. Klose, R. J., Kallin, E. M. & Zhang, Y. (2006). JmjC-domain-containing proteins and histone demethylation. *Nat. Rev. Genet.* **7**, 715–727.
4. Horton, J. R., Upadhyay, A. K., Qi, H. H., Zhang, X., Shi, Y. & Cheng, X. (2010). Enzymatic and structural insights for substrate specificity of a family of jumonji histone lysine demethylases. *Nat. Struct. Mol. Biol.* **17**, 38–43.
5. Fortschegger, K., de Graaf, P., Outchkourov, N. S., van Schaik, F. M., Timmers, H. T. & Shiekhattar, R. (2010). PHF8 targets histone methylation and RNA polymerase II to activate transcription. *Mol. Cell Biol.* **30**, 3286–3298.
6. Kleine-Kohlbrecher, D., Christensen, J., Vandamme, J., Abarrategui, I., Bak, M., Tommerup, N. *et al.* (2010). A functional link between the histone demethylase PHF8 and the transcription factor ZNF711 in X-linked mental retardation. *Mol. Cell*, **38**, 165–178.
7. Feng, W., Yonezawa, M., Ye, J., Jenuwein, T. & Grummt, I. (2010). PHF8 activates transcription of rRNA genes through H3K4me3 binding and H3K9me1/2 demethylation. *Nat. Struct. Mol. Biol.* **17**, 445–450.
8. Yokoyama, A., Okuno, Y., Chikanishi, T., Hashiba, W., Sekine, H., Fujiki, R. & Kato, S. (2010). KIAA1718 is a histone demethylase that erases repressive histone methyl marks. *Genes Cells*, **15**, 867–873.
9. Huang, C., Xiang, Y., Wang, Y., Li, X., Xu, L., Zhu, Z. *et al.* (2010). Dual-specificity histone demethylase KIAA1718 (KDM7A) regulates neural differentiation through FGF4. *Cell Res.* **20**, 154–165.
10. Liu, W., Tanasa, B., Tyurina, O. V., Zhou, T. Y., Gassmann, R., Liu, W. T. *et al.* (2010). PHF8 mediates histone H4 lysine 20 demethylation events involved in cell cycle progression. *Nature*, **466**, 508–512.
11. Qi, H. H., Sarkissian, M., Hu, G. Q., Wang, Z., Bhattacharjee, A., Gordon, D. B. *et al.* (2010). Histone H4K20/H3K9 demethylase PHF8 regulates zebrafish brain and craniofacial development. *Nature*, **466**, 503–507.
12. Wen, H., Li, J., Song, T., Lu, M., Kan, P. Y., Lee, M. G. *et al.* (2010). Recognition of histone H3K4 trimethylation by the plant homeodomain of PHF2 modulates histone demethylation. *J. Biol. Chem.* **285**, 9322–9326.
13. Ayoub, N., Noma, K., Isaac, S., Kahan, T., Grewal, S. I. & Cohen, A. (2003). A novel jmjC domain protein modulates heterochromatization in fission yeast. *Mol. Cell Biol.* **23**, 4356–4370.
14. Trewick, S. C., McLaughlin, P. J. & Allshire, R. C. (2005). Methylation: lost in hydroxylation? *EMBO Rep.* **6**, 315–320.
15. Elkins, J. M., Hewitson, K. S., McNeill, L. A., Seibel, J. F., Schlemminger, I., Pugh, C. W. *et al.* (2003). Structure of factor-inhibiting hypoxia-inducible factor (HIF) reveals mechanism of oxidative modification of HIF-1α. *J. Biol. Chem.* **278**, 1802–1806.
16. Tsukada, Y., Fang, J., Erdjument-Bromage, H., Warren, M. E., Borchers, C. H., Tempst, P. & Zhang, Y. (2006). Histone demethylation by a family of JmjC domain-containing proteins. *Nature*, **439**, 811–816.
17. Tahiliani, M., Mei, P., Fang, R., Leonor, T., Rutenberg, M., Shimizu, F. *et al.* (2007). The histone H3K4 demethylase SMCX links REST target genes to X-linked mental retardation. *Nature*, **447**, 601–605.
18. Iwase, S., Lan, F., Bayliss, P., de la Torre-Ubieta, L., Huarte, M., Qi, H. H. *et al.* (2007). The X-linked mental retardation gene SMCX/JARID1C defines a family of histone H3 lysine 4 demethylases. *Cell*, **128**, 1077–1088.
19. Han, Z., Liu, P., Gu, L., Zhang, Y., Li, H., Chen, S. & Chai, J. (2007). Structural basis for histone demethylation by JHDM1. *Frontier Sci.* **1**, 52–67.
20. Feng, W. (2009). The Jumonji domain containing proteins PHF2 and PHF8 act in concert to stimulate transcription of rRNA genes. Dissertation (under Prof. Dr. Ingrid Grummt), University Heidelberg, Germany (http://www.ub.uni-heidelberg.de/archiv/9945).

21. Frescas, D., Guardavaccaro, D., Bassermann, F., Koyama-Nasu, R. & Pagano, M. (2007). JHDM1B/FBXL10 is a nucleolar protein that represses transcription of ribosomal RNA genes. *Nature*, **450**, 309–313.
22. Li, F., Huarte, M., Zaratiegui, M., Vaughn, M. W., Shi, Y., Martienssen, R. & Cande, W. Z. (2008). Lid2 is required for coordinating H3K4 and H3K9 methylation of heterochromatin and euchromatin. *Cell*, **135**, 272–283.
23. Chang, B., Chen, Y., Zhao, Y. & Bruick, R. K. (2007). JMJD6 is a histone arginine demethylase. *Science*, **318**, 444–447.
24. Webby, C. J., Wolf, A., Gromak, N., Dreger, M., Kramer, H., Kessler, B. *et al.* (2009). Jmjd6 catalyses lysyl-hydroxylation of U2AF65, a protein associated with RNA splicing. *Science*, **325**, 90–93.
25. Mantri, M., Krojer, T., Bagg, E. A., Webby, C. J., Butler, D. S., Kochan, G. *et al.* (2010). Crystal structure of the 2-oxoglutarate- and Fe(II)-dependent lysyl hydroxylase JMJD6. *J. Mol. Biol.* **401**, 211–222.
26. Hong, X., Zang, J., White, J., Wang, C., Pan, C. H., Zhao, R. *et al.* (2010). Interaction of JMJD6 with single-stranded RNA. *Proc. Natl Acad. Sci. USA*, **107**, 14568–14572.